Journal of King Saud University – Science 34 (2022) 101837

Contents lists available at ScienceDirect

Journal of King Saud University – Science

journal homepage: www.sciencedirect.com

Original article

The predicted models of anti-colon cancer and anti-hepatoma activities of substituted 4-anilino coumarin derivatives using quantitative structure-activity relationship (QSAR)

Daratu Eviana Kusuma Putri [a,*], Harno Dwi Pranowo [b], Anugrah Ricky Wijaya [a], Novia Suryani [c], Maisari Utami [d], Artania Adnin Tri Suma [e], Woo Jin Chung [f], Saeedah Musaed Almutairi [g], Dina S. Hussein [h], Rabab Ahmed Rasheed [i], Venkatalakshmi Ranganathan [j,*]

[a] Department of Chemistry, Universitas Negeri Malang (UM) or State University of Malang, Jl. Semarang 5 Malang, 65145, Indonesia
[b] Department of Chemistry, Faculty of Mathematics and Natural Sciences, Universitas Gadjah Mada, Jl. Sekip Utara, Yogyakarta 55281, Indonesia
[c] Department of Chemistry, Universitas Islam Negeri Mataram, Jl. Gajah Mada No. 100, Mataram 83116, Indonesia
[d] Department of Chemistry, Universitas Islam Indonesia, Jl. Kaliurang km. 14.5, Sleman 55584, Indonesia
[e] Department of Pharmaceutical Chemistry, Faculty of Pharmacy, Universitas Gadjah Mada, Jl. Sekip Utara, Yogyakarta 55281, Indonesia
[f] Department of Environmental Energy and Engineering, Kyonggi University, Youngtong-Gu, Suwon, Gyeonggi-Do 16227, Republic of Korea
[g] Department of Botany and Microbiology, College of Science, King Saud University, Riyadh 11451, Saudi Arabia
[h] Department of Chemistry, College of Sciences and Health, Cleveland State University, Cleveland 44115, USA
[i] Histology & Cell Biology Department, Faculty of Medicine, King Salman International University, South Sinai, Egypt
[j] Faculty of Pharmaceutical Sciences, UCSI University, 56000 Cheras, Kulala Lumpur, Malaysia

ARTICLE INFO

Article history:
Received 30 August 2021
Revised 29 December 2021
Accepted 12 January 2022
Available online 28 January 2022

Keywords:
Coumarin
Anti-cancer
QSAR
MLR

ABSTRACT

Objectives: The objective of this work was to predict anti-colon and anti-hepatoma cancer activity of newly designed substituted 4-anilino coumarin derivatives using quantitative structure–activity relationship (QSAR).
Methods: The optimization of the derivatives including molecular and electronic properties data to generate the QSAR were resulted from H-GGA DFT/BPV86 method calculation combined with Hartree-Fock 6-31G basis set. The QSAR models were delivered in multiple linear regression (MLR) and the drug design was accomplished by considering the descriptors constructing the best QSAR models for each biological activity.
Results: This research accomplished two best validated QSAR models for predicting anti-colon cancer and anti-hepatoma activities of substituted 4-anilino coumarin derivatives. There were 17 of newly designed substituted 4-anilino coumarin derivatives which their anticancer activity (Log IC_{50}) were predicted using our both QSAR models. The QSAR predictions inform that the compound 25 and compound 19 have the best predicted anti-colon cancer and anti-hepatoma activities, respectively.
Conclusion: The results revealed that this approach can be used to assist in the action of anticancer drug discovery. Moreover, the retrosynthesis analysis of both compounds are also explained in a logic reverse of organic synthetic steps through Knoevenagel and Perkin reactions.

1. Introduction

Worldwide, cancer is one of seven leading death causes in more and less economically developed countries (Torre et al., 2015). Colon cancer and hepatocellular carcinoma are included as the most common human malignant diseases with the highest death cases (Ma et al., 2020). One of the most popular treatment of liver disease in early stage is liver transplantation but unfortunately it is limited to the lack of donors (Reddy et al., 2013). Thus, chemotherapy remains the main strategy for cancer treatment, but the

* Corresponding authors.
E-mail addresses: daratu.putri.fmipa@um.ac.id (D. Eviana Kusuma Putri), rvenkatmpharm@gmail.com (V. Ranganathan).
Peer review under responsibility of King Saud University.

Production and hosting by Elsevier

https://doi.org/10.1016/j.jksus.2022.101837
1018-3647/

phenomenon of drug resistance and the emergence of minimal side effect from new anti-cancer agents (Ma et al., 2020) are being the essential intention for cancer chemotherapy.

The propitious biological activity and simple synthetic modification have brought the scientists to design and develop the coumarin derivatives as pharmaceutical compounds (Cao et al., 2016). They exhibit variance biological activities such as anticoagulants (Horak et al., 2018), antidepressant (Sashidhara et al., 2011), antitumor (Cao et al., 2016), antioxidant (Erzincan et al., 2015) and so on. Cao et al. (2016) synthesized coumarin which exhibited potent anti-proliferative ability causing G2/M phase arrest. They claimed that this excellent activity came from the *N*-methyl linker group in coumarin hybrid. Luo et al. had synthesized coumarin scaffold and aniline moieties (substituted 4-anilino-coumarin derivatives) (Luo et al., 2017) which were *in vitro* cytotoxic activity evaluated against four human cancer cell lines (MCF-7, HepG2, HCTI16, and Panc-1). The effect of cell cycle arrest was assayed to MCF-7 (human breast cancer cell line) for the best compound which proving into concentration-dependently to ruin cell cycle at G2/M phase. Further, Luo *et al.* evaluated the best compound for the cytotoxicity test against HUVEC (human umbilical vein endothelial cells) which revealed normal cells were far less sensitive to the assayed compounds over cancer cells.

Quantitative Structure-Activity Relationship (QSAR) approach take the role to correlate the biological activity of compounds group with the computated molecular properties (Amin et al., 2021). Mladenovic *et al.* had used multiple linear regression (MLR) to perform the correlation between the antioxidant activity and various molecular descriptors (Mladenović et al., 2011). They employed DFT/B3LYP functional and 6-31G basis set to optimize the derivatives using Gaussian 03 software. Other research, Erzincan et al. (2015) created the QSAR equation and revealed that some physicochemical characters such as H-bond donor and lipophilic were important parameters in describing antioxidant ability.

QSAR modelling usually consists of four main steps: computing a series of descriptors, selecting some relevant descriptors, building the frequent nonlinear relationship between the descriptors and the biological activity, and validating the model.

$$\text{Biological activity} = c_0 + c_1 d_1 + c_2 d_2 + \ldots \quad \text{(II.1)}$$

2. Materials and methods

2.1. Hardware and software

The research used a PC with CPU @ 2.00 GHz RAM 4.00 GB Intel® Core™ i3-5005U. The softwares utilized were Hyperchem™ 8.0.10, Gaussian® 09 W, IBM® SPSS® Release 23, and ACD/ChemSketch 14.0. Overall research was being done at Austrian-Indonesian Centre for Computational Chemistry (AIC) Laboratory, Department Chemistry, Faculty of Mathematics and Science, Universitas Gadjah Mada.

2.2. Materials

A data set of 27 compounds (Luo et al., 2017) was used to generate the QSAR equations. The anticancer activity data were set as dependent variables (IC_{50}) to HCT116 and HepG2 (μM) which were modified into logarithmic.

2.3. Method of calculation

Compound **33d** as the most-desiring-activity compound was computed using PM6, DFT/BPV86, DFT/PBE, DFT/B3LYP (Van Bay et al., 2021), and Hartree-Fock (HF) method (Hmamouchi et al., 2016). The Basis set applied for HF and DFT calculation was 6-31G. ^{13}C NMR chemical shifts were calculated by DFT/B3LYP method and 6-31G basis set. The best method with low correlation error between experimental and calculated chemical shift was selected.

2.4. Geometrical optimization and descriptors calculation

The 27 compounds of substituted 4-anilino coumarin derivatives were depicted employing GaussView 5.0 and optimized by Gaussian 09W application. From the calculations, E_{LUMO}, E_{HOMO}, delta E_{HOMO}-E_{LUMO} (ΔE), atomic charge (q), and dipole moment (μ) were obtained. The rest descriptors, volume (V), molecular mass (MW), refractivity (MR), partition coefficient (log P), polarisability (α), and surface area (SA) were calculated using Hyperchem™ 8.0.10.

2.5. Model development and validation

QSAR equations were created by utilizing multiple linear regression (MLR) using IBM® SPSS® Release 23. The regression development method was backward elimination with confident interval level 95%. The internal validation should meet the significance test: $r^2_{train} > 0.6$ (Golbraikh and Tropsha, 2000), SEE < 0.3 (Mishra et al., 2014), test $F_{cal}/F_{tab} > 1$, $\alpha(0.05) > sig(0.00)$ (Pramesti, 2017). The external validation used to eliminate the unqualified equations, $r^2_{test} > 0.6$, $r^2_{overall} > 0.5$, and $RMSE_{test} < 0.3$ are critical to be calculated (Golbraikh and Tropsha, 2000).

2.6. Drug design

The drug design was done by replacing the R_1, R_2, and R substituents from coumarin derivatives. Hydrophobic, electronic, and steric effects were the main properties to consider. To attain proper hydrophobic character, log P, R_1, R_2, and R of the newly designed molecules were replaced with certain moieties. To avoid unwanted value of Log P, Lipinski's "rule of five" was implemented.

3. Results and discussion

3.1. Method of calculation

The compound used was **33d** that was 4-(1,3-benzodioxol-5-yla mino)-6-methoxy-3-(trifluoroacetyl)–2*H*-chromen-2-one as it had the pre-eminent anti-cancer activity among the listed derivatives (Luo et al., 2017). In Fig. S1 (see the figure in Supplementary material), HF/6-31G method performs significant inaccuracy to predict the ^{13}C NMR spectra than DFT and semiempirical method. High degree of error is proved by its high RMSE calculation which is 15.79 and low linearity between experimental and calculated chemical shifts was showed by r^2 (0.9785) (Putri et al., 2019). This lack might due to this method's limitation to carry the electron correlation in calculation process (Young, 2001). Electron correlation is important to improve the accuracy of computed energies and molecular geometries (Piris, 2017).

Semiempirical method (PM6 method) has better result than HF method expressed by higher r^2 that is 0.9908. But, this method gives higher RMSE value (13.08) compared with several DFT methods indicates the higher error. The sp^3 hybridization of nitrogen in the derivatives can be the main cause of false prediction from PM3 or AM1 calculation (Clark, 1993).

From Fig. S1, it can be seen that the three closest theoretical chemical shifts to the experiment are all from DFT methods (BPV86, PBE, and B3LYP). DFT functionals verily rely on organic compounds molecular structure (Van Bay et al., 2021). The deter-

mination coefficient of the three DFT functionals are 0.9834 (BPV86) (Putri et al., 2019), 0.9825 (PBE), and 0.9812 (B3LYP) indicating the pleasant coherence between theoretical and experimental chemical shifts. B3LYP RMSE calculation gives higher value comparing with PBE and BPV86. Despite, PBE method provides negligible difference in RMSE calculation (9.52) with BPV86 (9.27) (Putri et al., 2019) but its optimizing process is significantly more time consuming. Therefore, DFT/BPV86 using 6-31G basis set is the best method which offers the best prediction for the independent variables to be more accurate. In addition, BPV86 is included as hybrid GGA (generalized gradient approximation) functional (Sajjad et al., 2017) which integrate Becke and Perdew's 1986 functional density with electron correlation replaced with Vosko.

3.2. Geometrical optimization and descriptors calculation

Generating QSAR equations always charge high attentions in the entire process. The Hartree-Fock complicity in Hybrid density functional (H-GGA) methods upgrades a conventional GGA used in this research (BPV86) into the next level sophistification for the derivatives. H-GGA let a percentage of Hartree-Fock exchange to be fitted semiempirically with experimental ionization potentials, total atomic energies, proton affinities and other data representating a group of small molecules (Becke, 1993).

The data of several distance modifications between two atoms are performed in Table S1 (see the table in Supplementary material). The distance between C_7 and O without optimization is quite narrow (1.338 Å). Following the optimization, the distance becomes wider (1.412 Å) placing the atoms into more relax position and reduce the high level energy.

3.3. Model development and validation

The QSAR equations robustness is predicted by calculating the capability of the training set equation to predict log IC_{50} of the test set. Backward elimination has become the most promising method to progressively eliminate the descriptors and also gives better performance to correlation coefficient compared with forward selection and stepwise regression. In the end of the process, only a few descriptors are left in order to reduce redundant, the risk of overfitting from noisy and irrelevant descriptors.

3.4. Model development and validation of anti-colon cancer (anti-HCT)

The best five models resulted from various training and test set packs of anti-colon cancer activity are listed in Table S2 (see the table in Supplementary material). The lowest r_{train} value is 0.872 and the lowest r^2_{train} is 0.760. It explains the goodness of statistical

Table 1
External statistical validation of QSAR models of anti-colon cancer activity resulted by MLR.

Model	Test set	r^2_{test}	PRESS	RMSE
1	23e, 14f, 23f, 23a, 14a	0.5398	1.940	0.623
2	14e, 33b, 14f, 23a, 23i	0.6033	0.217	0.208
3	14e, 33b, 14f, 23a, 23i	0.8216	0.217	0.208
4	32c, 33b, 23f, 14i, 25c	0.8307	0.157	0.177
5	32c, 14e, 14a, 14c, 14g	0.8508	0.277	0.336

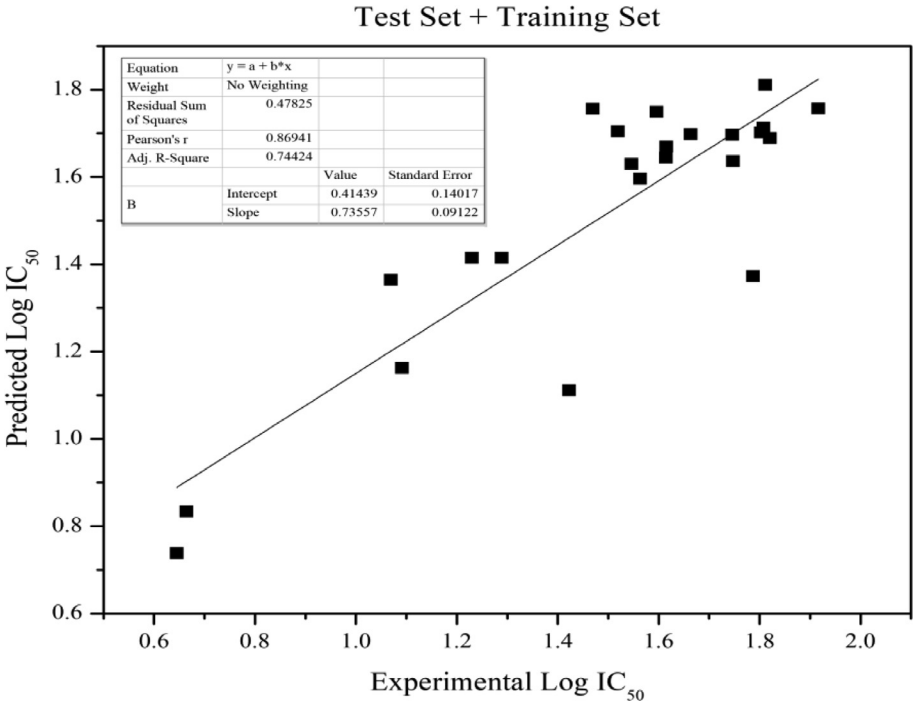

Fig. 1. The correlation of experimental and predicted Log IC_{50} of anti-HCT training and test set.

Table 2
Developed QSAR models of anti-hepatoma activity resulted by MLR.

Model	Test set	r^2	PRESS	RMSE
1	14b, 23b, 25a, 25d, 25e	0.6394	0.639	0.358
2	14b, 23b, 25a, 25d, 25e	0.8223	0.445	0.298
3	14a, 14e, 23b, 23e, 25c	0.6905	1.376	0.525
4	14b, 14g, 23b, 23g, 25d	0.4912	1.825	0.604
5	14e, 23e, 32c, 33b, 33e	0.3052	3.781	0.870

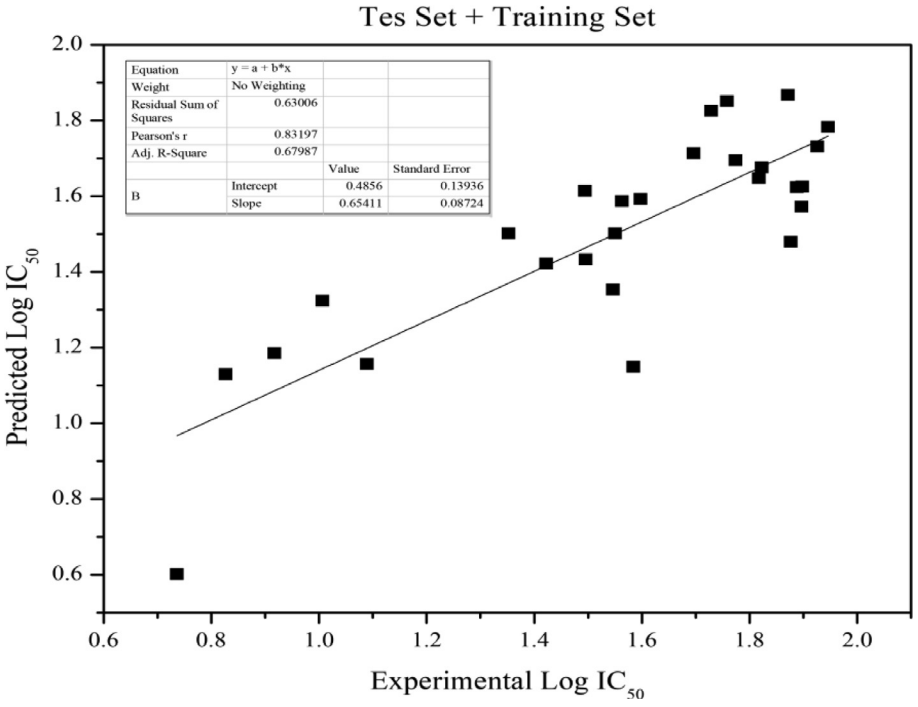

Fig. 2. The correlation of experimental and predicted Log IC_{50} of anti-hepatoma training and test set.

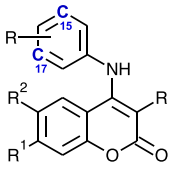

$$\text{Log } IC_{50} = 0.767 + (-1.768 \times qC_{15}) + (2.182 \times qC_{17}) + (0.208 \times \text{Log P}) \quad \textbf{(Eq.1)}$$

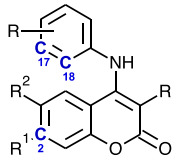

$$\text{Log } IC_{50} = 0.34 + (0.717 \times qC2) + (1.012 \times qC17) + (4.961 \times qC18) + (0.385 \times \text{Log P}) \quad \textbf{(Eq. 2)}$$

Fig. 3. Atomic charge points of each equation.

significance that is>87.2% and the r^2_{train} reveals the closeness of the data to the fitted regression. This study provided the lowest F_{cal}/F_{tab} values of all models is 3.588 explaining a good statistically significant. Every model is clustered as having good accuracy in predicting Log IC_{50} of anti-HCT.

The external validation was done. In Table 1, the data which satisfied the standard were merely model 4. Model 4 presented r^2_{test} 0.8307, with RMSE 0.177, and PRESS 0.157. The PRESS and RMSE value of this model was occupied as the smallest value considering that model 4 gave the least error. In addition, the accuracy of the model 4 was described by correlation coefficient (r = 0.882) that meant statistical significance>88% (Fig. S3, see the figure in Supplementary material). Therefore, model 4 was considered as a validated, robust, and predictive model. (Model 4, Table S2)

$$\text{Log } IC_{50} = 0.767 + (-1.768 \times qC_{15}) + (2.182 \times qC_{17}) + (0.208 \times \text{Log P}) \quad (1)$$

$n = 23$; $r^2_{train} = 0.778$; $r^2_{test} = 0.8307$ $r^2_{overall} = 0.7559$; $F_{cal}/F_{tab} = 4.890$; SEE = 0.193

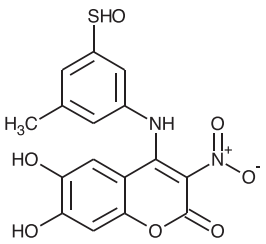

11
IC_{50} HCT = 7.33 µM
IC_{50} HEP = 40.29 µM

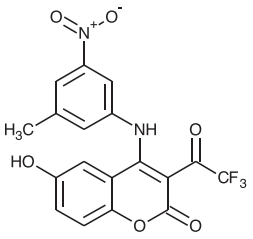

12
IC_{50} HCT = 18.73 µM
IC_{50} HEP = 17.27 µM

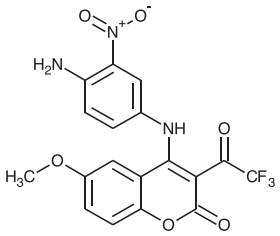

13
IC_{50} HCT = 2.44 µM
IC_{50} HEP = 3.46 µM

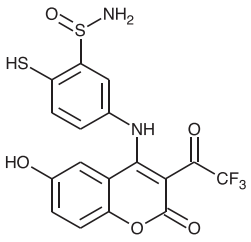

14
IC_{50} HCT = 45.46 µM
IC_{50} HEP = 6.87 µM

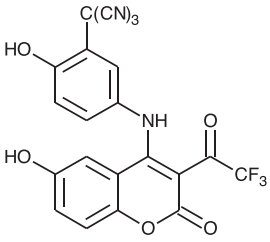

15
IC_{50} HCT = 10.73 µM
IC_{50} HEP = 6.73 µM

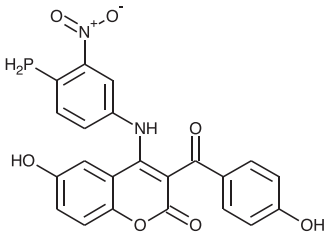

16
IC_{50} HCT = 7.30 µM
IC_{50} HEP = 29.59 µM

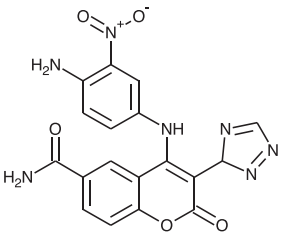

17
IC_{50} HCT = 0.99 µM
IC_{50} HEP = 1.13 µM

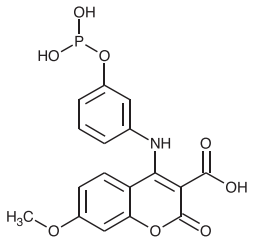

18
IC_{50} HCT = 42.32 µM
IC_{50} HEP = 19.64 µM

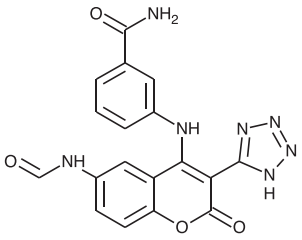

19
IC_{50} HCT = 3.41 µM
IC_{50} HEP = 0.44 µM

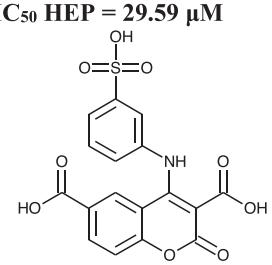

20
IC_{50} HCT = 274.14 µM
IC_{50} HEP = 345.24 µM

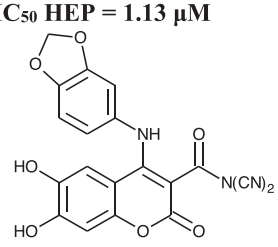

21
IC_{50} HCT = 3.28 µM
IC_{50} HEP = 3.44 µM

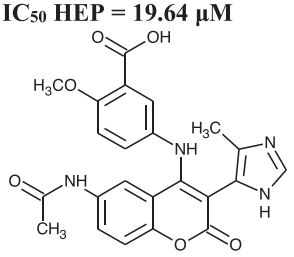

22
IC_{50} HCT = 6.32 µM
IC_{50} HEP = 1.79 µM

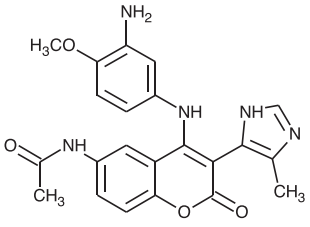

23
IC_{50} HCT = 1.73 µM
IC_{50} HEP = 0.82 µM

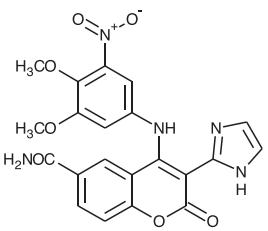

24
IC_{50} HCT = 18.80 µM
IC_{50} HEP = 5.22 µM

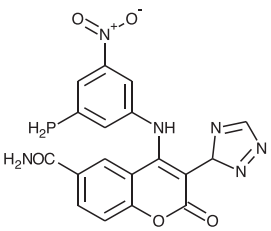

25
IC_{50} HCT = 0.82 µM
IC_{50} HEP = 1.11 µM

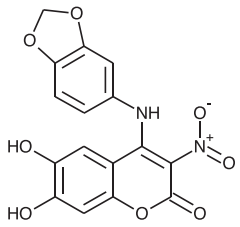

26
IC_{50} HCT = 4.12 µM
IC_{50} HEP = 3.73 µM

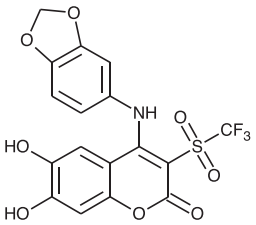

27
IC_{50} HCT = 33.26 µM
IC_{50} HEP = 202.29 µM

Fig. 4. New compound designs.

The descriptors that affect the molecule's activities are C15 and C17 of anilino group and Log P (Eq. 1, Fig. 3). This discovery is suitable with molecular docking of Cao *et al.* which shows that anilino forms hydrophobic interactions with amino acids residues Ala316 (Cao et al., 2016). The atomic charge shift significantly changes the interaction ability of this ring with its receptor. Another critical factor was the solubility. Unsatisfactory log P of a drug may cause it never reach the receptor. The calculated log IC_{50} values of model 4 of all compounds were compared with the experimental activities giving a slope of 0.7559 that shows that this model is able to favourably predict 75.59% of the data (Fig. 1).

3.5. Model development and validation of Anti-Hepatoma activity (anti-HEP)

Table S3 (see the table in Supplementary material) provides the best models of various training and test sets for anti-hepatoma activity resulted by SPSS software. The lowest r values is 0.845 indicating a good statistical significance which is >84.5%. Every model in Table S3 shows a very good determination coefficient that the lowest is 0.747. The other case, the whole ratio values of F_{cal}/F_{tab} show numbers between 3.588 and 7.400 which meet the standard value. In addition, the highest SEE value among all candidate is 0.209 meaning the errors rate of all equation are quite small.

The external validation was done which model 1, 2, and 3, presented r^2_{test} > 0.6 (Table 2). Yet, the only accepted RMSE value was belonged to model 2 that was 0.298. This model also had the smallest PRESS values (0.445). The both values meant that its error was the mildest among the rest equations. Despite, the r^2_{test} (0.8223) occupied as the highest r^2_{test} among others. In addition, model 2 has statistical significance >86% (Fig. S5, see the figure in Supplementary material). Therefore, model 2 was considered as a robust, validated and predictive model.

The descriptors that affect the molecules activities are C2, C17, C18 and Log P. C17 and C18 build the anilino ring (Eq. 2, Fig. 3). According to Cao *et al.*, this anilino ring is very important for derivative's anticancer activity due to its hydrophobic interaction with amino acid Ala316. (Model 2, Table S3)

$$\text{Log } IC_{50} = 0.34 + (0.717 \times qC2) + (1.012 \times qC17) + (4.961 \times qC18) + (0.385 \times \text{Log P}) \quad (2)$$

$$n = 27;\ r^2_{train} = 0.747;\ r^2_{test} = 0.8223\ r^2_{overall} = 0.6922$$

$$F_{cal}/F_{tab} = 4.249;\ SEE = 0.197$$

Log P descriptor could be further modified to provide better anticancer activity. The picture above was the comparison between calculated log IC_{50} from entire derivatives and observed values providing r^2 = 0.6922. This determination coefficient indicates that the model was able to favourably predict 69.22% of the data (Fig. 2).

3.6. Drug design

Analyzing Eqs. 1 and 2, hydrophobic and electronic were the physicochemical properties that should be further discussed. The hydrophobic properties of a drug is vital to provide it's easiness to cross cell membranes and in receptor interaction. Despite, a huge part of all living mass consists of water leading to every biochemical reactions are in aqueous phase. The new molecules should have certain moieties that alter the Log P becoming lower than the reference yet maximize its performance to cross lipid bar-

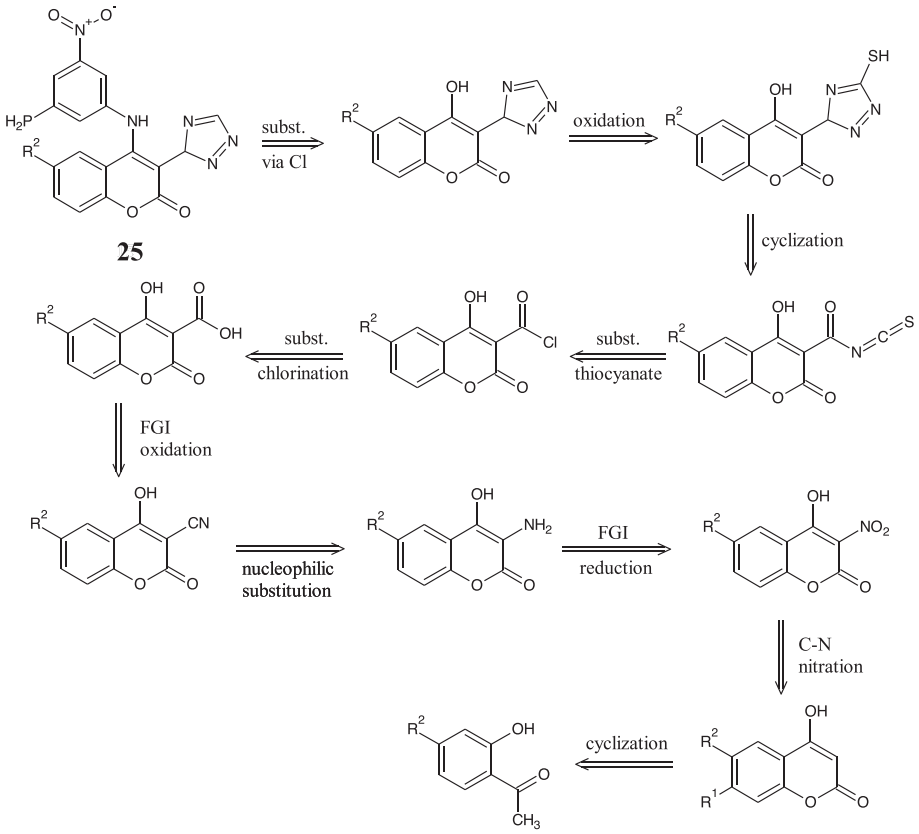

Fig. 5. Retrosynthesis of new designed compound **25.**

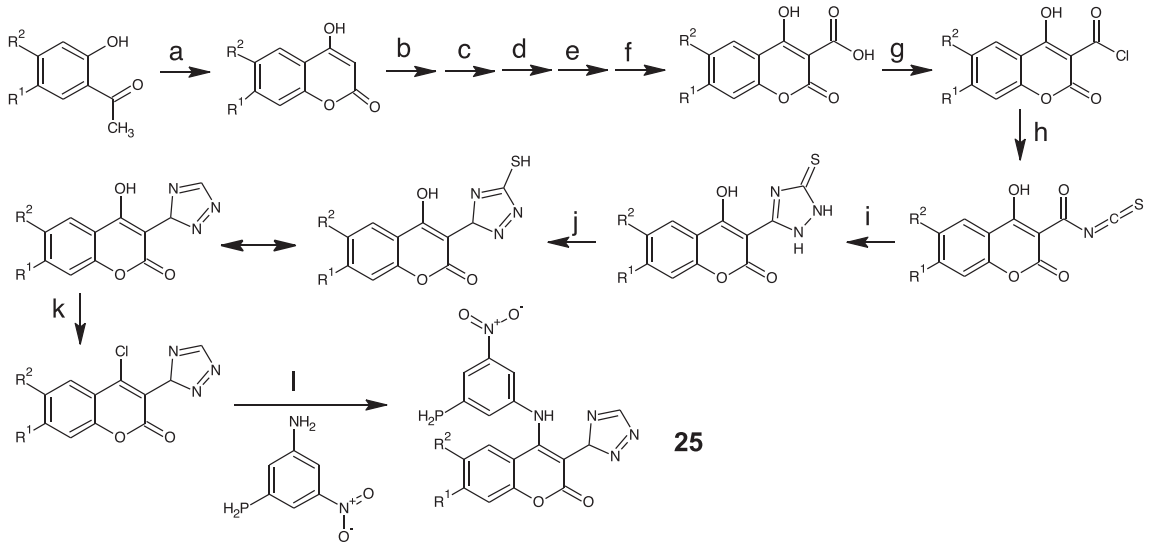

Fig. 6. Reagents and conditions of new anti-coloncancer compound (**25**) synthesis:(a) NaH, DEC, 120 °C, 3 h; (b) HNO_3, H_2SO_4 (c) H_2, Pd, C, Ac_2O; (d) HCl, H_2O; (e) HCl, $NaNO_2$, Cu(I)CN; (f) NaOH; (g) $SOCl_2$; (h) NH_4SCN; (i) N_2H_4; (j) HNO_3, H_2O, 45 °C; (k) $POCl_3$, 60 °C, 2 h; (l) K_2CO_3, DMF, 75 °C, 2 h. (Luo et al., 2017; Godhani et al., 2015; Holm and Straub, 2011; Warren, 1982; Potts, 1961).

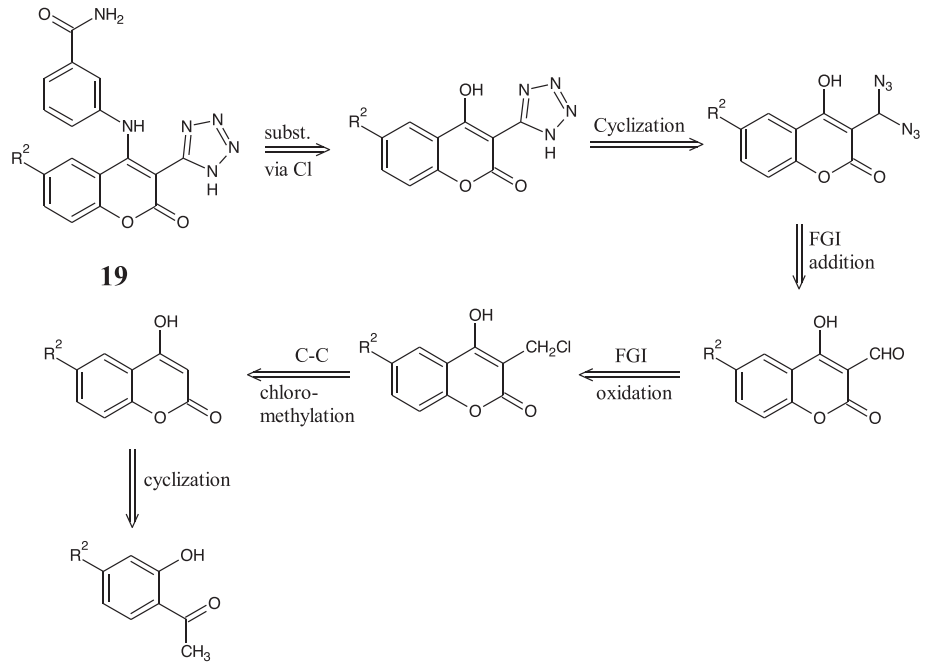

Fig. 7. Retrosynthesis of new designed compound **19.**

riers. Therefore, Lipinski's "rule of five" is also implemented to design new molecules.

A drug polarity is highly affected by the electronic. These characteristics give an effect on how easily a drug could pass cell membranes or how strongly it could bind to a receptor. According to Eqs. 1 and 2 (Fig. 3), the potential of the compounds is highly correlated with the partial atomic charge of the benzene rings. Hence, the moieties chosen to create new molecules with certain atomic charges. The overall result of new compound designs are presented in Fig. 4. The most promising structure for anti-coloncancer is structure **25** with a predicted IC_{50} = 820 nM and for anti-hepatoma is structure **19** with predicted IC_{50} = 440 nM.

The retrosynthesis of newly designed compounds 25 and 19 is depicted in Figs. 5 and 7 respectively. Referring to them, aniline from the lactone (coumarin) ring should be disconnected firstly. The disconnection gives aniline derivative and 4-chlorocoumarin (Godhani et al., 2015; Holm and Straub, 2011). The substitution is applied to be easily performed via chloride than hydroxyl due to hydroxyl's poor leaving group ability (Luo et al., 2017).

The pentagonal ring of 1,2,4-triazole can be made by nucleophilic substitution of thiocyanate into chloro-carbonyl moiety followed with cyclization and oxidation (Godhani et al., 2015). The carboxylation into coumarin ring cannot be easily made, therefore it needs an FGI from –CN. The last disconnection builds O_1-C_2 and

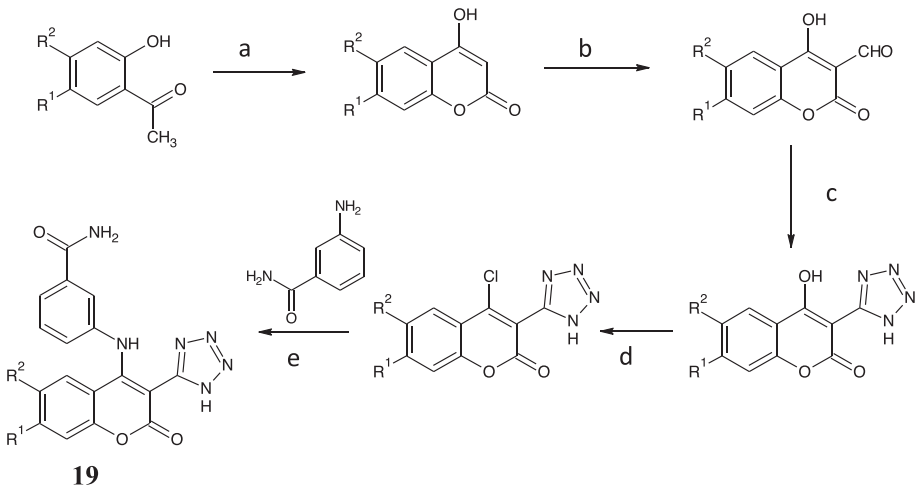

Fig. 8. Reagents and conditions of new anti-hepatoma compound (**19**) synthesis: (a) NaH, DEC, 120 °C, 3 h; (b) $ZnCl_2$, CH_2O, HCl; (c) $SiCl_4$, NaN_3, CH_3CN, 25 °C, 12 h; (d) $POCl_3$, 60 °C, 2 h; (e) K_2CO_3, DMF, 75 °C, 2 h (Luo et al., 2017; El-Ahl et al., 1995; Warren, 1982).

C_3-C_4 in the cyclic shape of the coumarin ring. The lactone ring cyclization requires an aromatic *o*-hydroxy carbonyl compound and a two-carbon fragment (C_2 and C_4 builder) in Knoevenagel and Perkin reactions. Despite, the reaction of aldehyde and triazide chlorosilane (TACS) was suggested via the formation of siloxy azide, and subsequent formation of gem-diazoalkane to give later cyclization to tetrazole derivatives (El-Ahl et al., 1995). These probable synthesis routes of the proposed compound has been completely written as Figs. 6 and 8.

Cancer treatment like chemotherapy have major limitations. Chemotherapy strategy is powerful in killing cancer cells but also has curing problems caused by cytotoxic side effects on normal cells (Hendouei et al., 2019). This research has considered this risk by selecting the main molecule skeleton with low toxicity towards normal human cells (HUVEC). It is highly recommended to follow any cancer regimens regulation from the medication institution including any involvement of antipsychotic drug to relieve nausea and other side effect of the treatment. Furthermore, for those who are at high risk of chemotherapy it is recommended to consider colonoscopy for colon cancer screening and surveillance to detect the colonic lesions before receiving any treatments.

4. Conclusions

The anti-colon cancer and antihepatoma activity of substituted 4-anilino coumarin derivatives were successfully predicted using QSAR equation of multiple linear statistical analysis. The validated QSAR models designed the 17 new compounds of substituted 4-anilino coumarin derivatives and predicted their anti-colon cancer and anti-hepatoma activities. The best new compounds, 4-[(3-nitro-5-phosphanylphenyl)amino]-2-oxo-3-(3*H*-1,2,4-triazol-3-yl)–2*H*-chromene-6-carboxamide was predicted as anti-colon cancer with IC_{50} = 0.82 μM, and 3-{[6-(formylamino)-2-oxo-3-(1*H*-tetrazol-5-yl)–2*H*-chromen-4-yl]amino}benzamide as anti-hepatoma with IC_{50} = 0.44 μM.

Declaration of Competing Interest

The authors declare that they have no known competing financial interests or personal relationships that could have appeared to influence the work reported in this paper.

Acknowledgments

We are grateful to Austrian-Indonesian Centre for Computational Chemistry (AIC) Laboratory, Department Chemistry, Faculty of Mathematics and Science, Universitas Gadjah Mada for providing their instrument facilities, PC, software computation for analysis data samples. The authors extend their appreciation to the Researchers supporting project number (RSP2022R470) King Saud University, Riyadh, Saudi Arabia.

Appendix A. Supplementary data

Supplementary data to this article can be found online at https://doi.org/10.1016/j.jksus.2022.101837.

References

Amin, S.A., Ghosh, K., Gayen, S., Jha, T., 2021. Chemical-informatics approach to COVID-19 drug discovery: Monte Carlo based QSAR, virtual screening and molecular docking study of some in-house molecules as papain-like protease (PLpro) inhibitors. J. Biomol. Struct. Dyn. 39 (13), 4764–4773. https://doi.org/10.1080/07391102.2020.1780946.

Becke, A.D., 1993. A new mixing of Hartree-Fock and local density-functional theories. J. Chem. Phys. 98 (2), 1372–1377. https://doi.org/10.1063/1.464304.

Cao, D., Liu, Y., Yan, W., Wang, C., Bai, P., Wang, T., Tang, M., Wang, X., Yang, Z., Ma, B., Ma, L., Lei, L., Wang, F., Xu, B., Zhou, Y., Yang, T., Chen, L., 2016. Design, Synthesis, and Evaluation of in Vitro and in Vivo Anticancer Activity of 4-Substituted Coumarins: A Novel Class of Potent Tubulin Polymerization Inhibitors. J. Med. Chem. 59 (12), 5721–5739. https://doi.org/10.1021/acs.jmedchem.6b00158.

Clark, T., 1993. Semiempirical Molecular Orbital Theory: Facts, Myths and Legends. In: Recent Experimental and Computational Advances in Molecular Spectroscopy. Springer Netherlands, Dordrecht, pp. 369–380. https://doi.org/10.1007/978-94-011-1974-0_21.

El-Ahl, A.-A., Elmorsy, S.S., Soliman, H., Amer, F.A., 1995. A facile and convenient synthesis of substituted tetrazole derivatives from ketones or α, β-unsaturated ketones. Tetrahedron Lett. 36 (40), 7337–7340. https://doi.org/10.1016/0040-4039(95)01513-H.

Erzincan, P., Saçan, M.T., Yüce-Dursun, B., Danış, Ö., Demir, S., Erdem, S.S., Ogan, A., 2015. QSAR models for antioxidant activity of new coumarin derivatives. SAR QSAR Environ. Res. 26 (7-9), 721–737. https://doi.org/10.1080/1062936X.2015.1088571.

Godhani, D.R., Jogel, A.A., Sanghani, A.M., Mehta, J.P., 2015. Synthesis and biological screening of 1, 2, 4-triazole derivatives. Ind. J. Chem. 54, 556–564.

Golbraikh, A., Tropsha, A., 2000. Predictive QSAR modeling based on diversity sampling of experimental datasets for the training and test set selection. Mol. Divers. 5, 231–243. https://doi.org/10.1023/A:1021372108686.

Hendouei, N., Saghafi, F., Shadfar, F., Hosseinimehr, S.J., 2019. Molecular mechanisms of anti-psychotic drugs for improvement of cancer treatment. Eur. J. Pharmacol. 856, 172402. https://doi.org/10.1016/j.ejphar.2019.05.031.

Hmamouchi, R., Larif, M., Chtita, S., Adad, A., Bouachrine, M., Lakhlifi, T., 2016. Predictive modelling of the LD 50 activities of coumarin derivatives using neural statistical approaches: electronic descriptor-based DFT. Integr. Med. Res. 10, 451–461. https://doi.org/10.1016/j.jtusci.2015.06.013.

Holm, S.C., Straub, B.F., 2011. Synthesis of N -substituted 1,2,4-triazoles. A review. Org. Prep. Proced. Int. 43 (4), 319–347. https://doi.org/10.1080/00304948.2011.593999.

Horak, K.E., Fisher, P.M., Hopkins, B., 2018. Pharmacokinetics of Anticoagulant Rodenticides in Target and Non-target Organisms 87–108. doi:10.1007/978-3-319-64377-9_4.

Luo, G., Muyaba, M., Lyu, W., Tang, Z., Zhao, R., Xu, Q., You, Q., Xiang, H., 2017. Design, synthesis and biological evaluation of novel 3-substituted 4-anilino-coumarin derivatives as antitumor agents. Bioorg. Med. Chem. Lett. 27 (4), 867–874. https://doi.org/10.1016/j.bmcl.2017.01.013.

Ma, L., Xu, G.B., Tang, X., Zhang, C., Zhao, W., Wang, J., Chen, H., 2020. Anti-cancer potential of polysaccharide extracted from hawthorn (Crataegus.) on human colon cancer cell line HCT116 via cell cycle arrest and apoptosis. J. Funct. Foods 64, 103677. https://doi.org/10.1016/j.jff.2019.103677.

Mishra, M., Mishra, V.K., Senger, P., Pathak, A.K., Kashaw, S.K., 2014. Exploring QSAR studies on 4-substituted quinazoline derivatives as antimalarial compounds for the development of predictive models. Med. Chem. Res. 23 (3), 1397–1405. https://doi.org/10.1007/s00044-013-0744-8.

Mladenović, M., Mihailović, M., Bogojević, D., Matić, S., Nićiforović, N., Mihailović, V., Vuković, N., Sukdolak, S., Solujić, S., 2011. In Vitro Antioxidant Activity of Selected 4-Hydroxy-chromene-2-one Derivatives—SAR, QSAR and DFT Studies. Int. J. Mol. Sci. 12, 2822–2841. https://doi.org/10.3390/ijms12052822.

Piris, M., 2017. Global method for electron correlation. Phys. Rev. Lett. 119,. https://doi.org/10.1103/PhysRevLett.119.063002 063002.

Pramesti, G., 2017. Statistika Penelitan dengan SPSS 24. PT. Gramedia, Jakarta.

Putri, D.E.K., Pranowo, H.D., Haryadi, W., 2019. Study on anti-tumor activity of novel 3-substituted 4 anilino-coumarin derivatives using quantitative structure-activity relationship (QSAR). Mater. Sci. Forum 948, 101–108. https://doi.org/10.4028/www.scientific.net/MSF.948.101.

Reddy, M.S., Varghese, J., Venkataraman, J., Rela, M., 2013. Matching donor to recipient in liver transplantation: Relevance in clinical practice. World J. Hepatol. 5 (11), 603. https://doi.org/10.4254/wjh.v5.i11.603.

Sajjad, S., Maria, Mahmood, T., Ayub, K., 2017. Benchmark study of structural and vibrational properties of scandium clusters. J. Mol. Struct. 1142, 139–147. https://doi.org/10.1016/j.molstruc.2017.04.046.

Sashidhara, K.V., Kumar, A., Chatterjee, M., Rao, K.B., Singh, S., Verma, A.K., Palit, G., 2011. Discovery and synthesis of novel 3-phenylcoumarin derivatives as antidepressant agents. Bioorg. Med. Chem. Lett. 21, 1937–1941. https://doi.org/10.1016/j.bmcl.2011.02.040.

Torre, L.A., Bray, F., Siegel, R.L., Ferlay, J., Lortet-Tieulent, J., Jemal, A., 2015. Global cancer statistics, 2012. CA. Cancer J. Clin. 65, 87–108. https://doi.org/10.3322/caac.21262.

Van Bay, M., Hien, N.K., Tran, P.T.D., Tuyen, N.T.K., Oanh, D.T.Y., Nam, P.C., Quang, D. T., 2021. TD-DFT benchmark for UV-Vis spectra of coumarin derivatives. Vietnam J. Chem. 59, 203–210. https://doi.org/10.1002/vjch.202000200.

Young, D.C., 2001. In: Chemistry Computational Chemistry a Practical Guide for Applying Techniques to Real-World Problems. New York. John Wiley & Sons, New York. https://doi.org/10.1002/jat.1666.